

Scaling Laws of Lissajous Acceleration for Electrodeless Helicon Plasma Thruster^{*})

Takeshi MATSUOKA, Ikkoh FUNAKI, Takahiro NAKAMURA¹⁾, Kenji YOKOI¹⁾,
Hiroyuki NISHIDA²⁾, Timofei S. RUDENKO³⁾, Konstantin P. SHAMRAI³⁾, Takao TANIKAWA⁴⁾,
Tohru HADA⁵⁾ and Shunjiro SHINOHARA²⁾

Japan Aerospace Exploration Agency, 3-1-1 Yoshinodai, Sagami-hara City, Kanagawa 252-5210, Japan

¹⁾*Graduate School of Engineering, Tokyo University of Agriculture and Technology,
2-24-16 Naka-cho, Koganei, Tokyo 184-8588, Japan*

²⁾*Institute of Engineering, Tokyo University of Agriculture and Technology,
2-24-16 Naka-cho, Koganei, Tokyo 184-8588, Japan*

³⁾*Institute for Nuclear Research, National Academy of Sciences of Ukraine, 47 Prospect Nauki, Kiev 03680, Ukraine*

⁴⁾*Research Institute of Science and Technology, Tokai University, 4-1-1 Kitakaname, Hiratsuka, Kanagawa 259-1292, Japan*

⁵⁾*Interdisciplinary Graduate School of Engineering Sciences, Kyushu University, 6-1 Kasuga Koen, Kasuga, Fukuoka
816-8580, Japan*

(Received 7 December 2010 / Accepted 4 March 2011)

Analytical thrust model for the Lissajous Helicon Plasma Accelerator (LHPA) is developed by extending previous works [1, 2] in order to guide experiments for achieving feasible value of the thrust. In the LHPA, a rotating transverse electric field in an external divergent magnetic field drives azimuthal currents via electron $\mathbf{E} \times \mathbf{B}$ drift then the thrust is produced due to the Lorentz force. One dimensional (1D) analytical model is developed which includes the electric field penetration into the plasma and the $\mathbf{E} \times \mathbf{B}$ current estimation based on a trajectory analysis. Thrust as a function of parameters of the plasma density and the magnetic field is studied. The penetration of the electrical field into plasmas is examined by 1D particle in cell (PIC) simulations whose results are consistent with those of the 1D analytical model.

© 2011 The Japan Society of Plasma Science and Nuclear Fusion Research

Keywords: Electrodeless thruster, Electric propulsion, Helicon plasma, Analytical model, PIC simulation

DOI: 10.1585/pfr.6.2406103

1. Introduction

Electric propulsions [3] in space applications have been used to save amount of propellants due to high specific impulse therefore enable to reduce the cost or time for various space missions. Successful thrusters such as ion or Hall thrusters have limited their lifetimes due to erosion of electrodes and charge neutralizers (Hollow cathodes). Several schemes are proposed for electrodeless thrusters with helicon plasma sources. Reference 4 is a recent review of electrodeless plasma thrusters. Helicon plasma sources are proposed for electrodeless thrusters because of the high density and its wide range of operation parameters [5, 6]. One of the electrodeless thruster is Lissajous Helicon Plasma Accelerator (LHPA) [1] in which the thrust is produced by the electromagnetic force (Lorentz force) and this is the uniqueness of this accelerator comparing with other thrusters: magnetic nozzle accelerators (VASIMR [7]) and static electric field accelerators (Double Layer [8]). Although acceleration of the axial plasma flow has been observed in experiments [1, 2, 8], ac-

celeration due to the Lorentz force has not yet been clearly observed. Therefore, a simple theoretical model which covers essential physics of the LHPA would be useful to guide experiments.

In this report, an analytical model for the thrust due to the Lorentz force in the LHPA and few guidelines for maximizing the Lorentz force, which may be relevant for experiments, are reported. Comparison between the model and PIC simulations for a key issue of electrical field penetration is given. The comparison of the results between the model and the PIC simulations shows quantitative agreement for degree of the electric field penetration. Physical processes which influence the thrust are discussed for future study.

2. Analytical Thrust Model

Figure 1 shows a configuration of the thruster. Plasma is generated by a helicon source (not shown in the figure) in a divergent magnetic field which is produced by a solenoid coil whose axis is in the z direction. The thrust is produced by the Lorentz force which is produced by the product of the azimuthal current and the radial magnetic field ($\mathbf{j}_\theta \times$

author's e-mail: takeshi.matsuoka1@gd.isas.jaxa.jp

^{*}) This article is based on the presentation at the 20th International Toki Conference (ITC20).

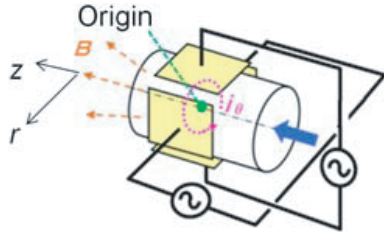
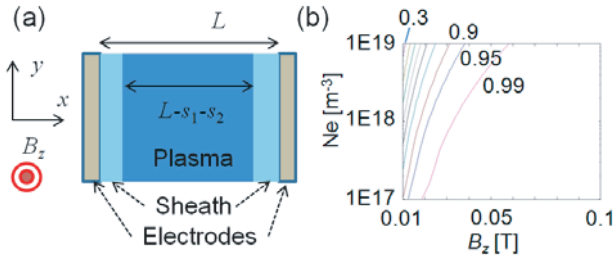


Fig. 1 Configuration of Lissajous Acceleration.


 Fig. 2 (a) Configuration of the REF penetration model. (b) Contour plot of penetrated REF by Eq. (3) for parameters of $V_0 = 100$ V, $r_0 = 0.05$ m, RF frequency ($f_{RF} = 1$ MHz). In Fig. 2 (b), contour interval is 0.1 between 0.3 and 0.9.

B_r) near the end of the solenoid. A key issue is how to produce the azimuthal current which is driven by a rotating electrical field (REF).

The REF vector lies in the transverse plane (\mathbf{E}_\perp) and rotates at a frequency of ω around the z axis. Selecting the applied frequency in a range specified by ω_{LH} (lower hybrid frequency) $\ll \omega \ll \omega_{ce}$ (electron cyclotron frequency) allows that immobile ion assumption thus electrons drift azimuthally via $\mathbf{E}_\perp \times \mathbf{B}_z$ drift motion. Here \mathbf{B}_z is the axial magnetic field. This electron drift is a source of the \mathbf{j}_θ [9]. Gyration motion of electrons also produces \mathbf{j}_θ (diamagnetic current). Solving the Newtonian motion equation in the REF and \mathbf{B}_z yields trajectories which consist of two circular motion whose radius are given by $R_D = E_\perp / \omega B_z$ and electron gyro radius (r_{ce}). The solenoid coil is modeled as a semi-infinite length whose end is placed at the origin ($z = 0$). An analytical expression of $B_r = B_z \cdot r/2a$ is used at the end of the solenoid coil. Here, a is the radius of the solenoid coil. This expression is accurate within 5% up to the half of the solenoid radius ($a/2$). In this report, all quantities are evaluated at $z = 0$.

Following the analysis given in [9], integration of individual electron trajectories for an axial symmetric density profile yields an expression for j_θ ,

$$j_\theta(r) = \frac{e}{2} (v_D R_D + v_{th} r_{ce}) \frac{\partial n(r)}{\partial r}. \quad (1)$$

Here, the drift velocity, the electron thermal velocity and the electron density are given by $v_D = E_\perp / B_z$, v_{th} and $n(r)$, respectively. Note that an inhomogeneous radial density profile is required to produce j_θ . Assuming a parabolic density profile with an expression given by $n(r) = n_0(1 -$

$\beta r^2 / r_0^2)$ in which β represents a measure of the density gradient and r_0 is the radius of the plasma. Averaging in the plasma cross section of radius r_0 yields an expression for the thrust (axial force) density in unit of N/m^3 ,

$$\langle f \rangle = \frac{e}{4} \beta n_0 \left(E_r \frac{r_0}{a} \frac{R_D}{r_0} + \frac{2k_\beta T_e}{ae} \right). \quad (2)$$

The k_β is the Boltzmann constant. The first (second) term is the thrust density due to the $\mathbf{E}_\perp \times \mathbf{B}_z$ drift motion (diamagnetic current). For fixed n_0 and \mathbf{E}_\perp , the thrust density is proportional to the R_D / r_0 but is limited by the two factors. First, when the ratio of R_D / r_0 approaches to 0.4, particle loss to the wall becomes significant since a considerable number of trajectories would intersect plasma boundary. In fact, a series of 2D PIC simulations showed that j_θ peaks at $R_D / r_0 \sim 0.4$ then decreases after the peak [9]. Thus the ratio should be kept smaller than ~ 0.4 . Second, a shielding of the REF due to electrons would limit the thrust density. Actually, second limitation is stronger than the first one for high density plasmas considered here (the electron density, $n_e > 10^{17} \text{ m}^{-3}$). The thrust density is proportional to the square of the E_\perp and n_0 when other parameters are fixed. Thus the strength of the REF is critical.

A 1D analytical model is developed for the REF field penetration in a configuration shown in Fig.2(a). The Poisson equation is solved, assuming continuity condition of the electric field. Plasma response is modeled by a uniform electron cold fluid with immobile ion background (charge neutralized bulk plasma) which is sandwiched by two planar electrodes. The distance between the electrodes is L and the thickness of the sheath are defined by $s_1(t)$ and $s_2(t)$ for the left- and the right-hand side sheathes, respectively. The REF is driven by setting a time varying potential at each electrodes, $V(t) = V_0 \sin(\omega t) / 2$ at the left electrode and $V(t) = -V_0 \sin(\omega t) / 2$ at the right electrode, respectively. The ion matrix sheath model ($n_e = 0$ in the sheath) is assumed. The thickness of the sheath [$s_1(t)$, $s_2(t)$] is obtained by solving the Newtonian motion equation for the electron fluid. In the 1D system, the total current (convection current + displacement current) is found to be constant throughout the system. When the amplitude of s_1 and s_2 becomes greater, the plasma current becomes greater since the total current in plasma is proportional to the amplitude. As a consequence, the displacement current, or equivalently the electric field in the plasma, becomes weaker. Collisions are neglected for the sake of simplicity. The solution of the REF, E_{p0} , in the bulk plasma is given by

$$\frac{E_{p0}}{V_0/L} = 1 - \frac{\text{sign}(\omega_{ce} - \omega)}{q} \left[\varepsilon - \sqrt{\varepsilon^2 + \text{sign}(\omega_{ce} - \omega) q} \right]^2, \quad (3)$$

with a dimensionless parameter of $q = 8eV_0\omega_{pe}^2 / mL^2\omega_{ce}^4$ and plasma dielectric function ($\varepsilon = 1 - \omega^2 / \omega_{ce}^2$) in the magnetized plasma. Details of the derivation of Eq.(3)

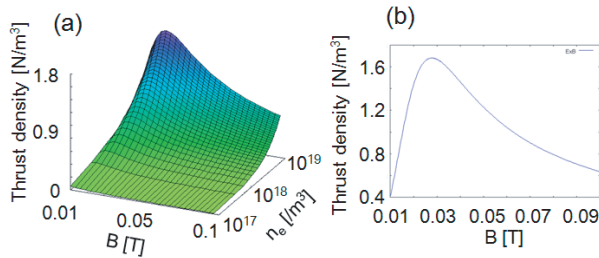


Fig. 3 Thrust density (a) in the $B - n_e$ plane and (b) as a function of the magnetic field at the fixed density of 10^{19} m^{-3} . Other parameters are $V_0 = 100 \text{ V}$, $r_0 = 0.05 \text{ m}$, RF frequency ($f_{\text{RF}} = 1 \text{ MHz}$), $\beta = 0.1$ and $a = 0.1 \text{ m}$.

in the present model will be reported in future. The term $\text{sign}(\omega_{ce} - \omega)$ is the sign of the $(\omega_{ce} - \omega)$. Here, ω_{pe} and m are the plasma frequency and the electron mass. Note that the REF strength is constant due to the charge neutrality of the bulk plasma. The REF strength is plotted in Fig. 2 (b) for a set of fixed parameters: r_0 , f_{RF} (or equivalently ω) and V_0 . The REF strength decreases when the plasma density increases due to a shielding by the plasma. The REF strength increases when the magnetic field increases due to reduction of the electron mobility. The influence due to the magnetic field is significant because of that the large area in the Fig. 2 (b) shows nearly 100% penetration ($E_{p0} \sim V_0/L$).

The thrust density can be estimated by substituting Eq. (3) into (2). Here, we neglected the diamagnetic current [the second term in Eq. (3)] in order to study the thrust density due to $\mathbf{E}_\perp \times \mathbf{B}_z$ drift. The thrust density is shown in Fig. 3 for the same parameters as in Fig. 2 (b). When the magnetic field is fixed, the thrust density increases with plasma density since the decrease of the REF strength is overcome by the increase of the plasma density. When the plasma density is fixed, the thrust density increases with the magnetic field until the peak of the thrust density (the optimum magnetic field). The thrust density decreases when the magnetic field is greater than the optimum magnetic field. The rise of the thrust density is explained by the increase of the REF strength due to reduced electron mobility. On the other hand, the fall of the thrust density in the region of the high magnetic field is due to decrease of R_D/r_0 , where R_D is inversely proportional to the magnetic field. Note that the REF strength is almost constant in the region.

3. PIC Simulations for REF Penetration

Among various issues in the thrust model, the REF strength from the model is compared with results from 1D PIC simulations by use of the VORPAL code [10]. The comparison is shown in Fig. 4. Dimensionless parameter of q is varied by changing the magnetic field for two densities. The other parameters in the simulations are $f_{\text{RF}} = 100 \text{ MHz}$ and $L = 1 \text{ cm}$. The numerical time step and the

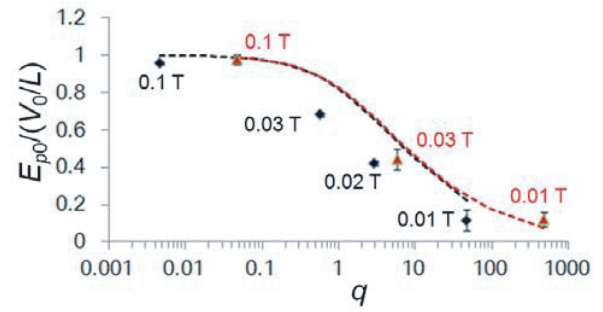


Fig. 4 REF strength as a function of q for a parameter set: $V_0 = 10 \text{ V}$, $L = 0.01 \text{ m}$, and $f_{\text{RF}} = 100 \text{ MHz}$. Simulation data points are shown for the plasma density of 10^{18} (10^{19}) m^{-3} by diamonds (triangles). The black (red) dotted curve shows REF strength from Eq. (3) for the plasma density of 10^{18} (10^{19}) m^{-3} . Strength of the magnetic field is shown in the plot.

spatial step are set at $1/10$ of the plasma wave period and the Debye length, respectively. The super particle number is varied from 200 (1,000) to 1,000 (10,000) for simulations at the density of 10^{18} (10^{19}) m^{-3} and the results are not affected by the number of the super particles. This indicates a negligible influence of numerical heating on simulation results. The Ar ions with a charge state of 1 along with a real mass ratio to the electron are used in the simulation. The ion and electron temperatures are 0.3 eV and 5 eV , respectively. Both energy distribution functions are assumed to be Maxwellian distribution as an initial condition. The REF in the simulation is obtained by a three-step post process.

First, the REF strength is spatially averaged between $0.05L$ and $0.95L$ in order to avoid the strong electric field in the sheath region. Second, the spatially averaged electric field is Fourier transformed to obtain a frequency spectrum. The spectrum shows a peak at the drive frequency (100 MHz) except for a data point at ($n_e = 10^{19} \text{ m}^{-3}$, $B_z = 0.01 \text{ T}$) where the intensity at the drive frequency is comparable with the intensity in the noise region described below. Third, the spectral peak is divided by the value which corresponds to electrical field (V_0/L) without the plasma. The error bar is estimated by taking averaged spectral intensity in a frequency range between 500 MHz to 1 GHz. The model curve is not sensitive to the difference of the plasma density. The REF strength decreases with the increase of the q . Note that the two theoretical curves overlapping each other since Eq. (3) does not depends on plasma density explicitly but q . However, q depends on plasma density and the density difference appears as different range of q in Fig. 4. Estimated values from PIC simulations show a good agreement with the model prediction. Therefore, we can conclude that Eq. (3) shows a key physics (REF shielding due to plasma electrons in magnetized plasma) in given assumptions.

4. Discussions

We discuss here five issues in the thrust evaluation. First, in generating the j_θ , a radially non uniform plasma density is required. However, in the REF penetration model, uniform plasmas are assumed. For a parabolic density profile which has a peak on axis as assumed in Eq. 2, the strength of REF increases from the value which is obtained in the constant plasma density. This increase is due to the decrease of the plasma density at the edge of the plasma. Despite of this inconsistency, the scaling law shows the essential physics for the thrust evaluation but the inconsistency can affect the absolute value. We selected a value of $\beta = 0.1$ in order to minimize this inconsistency. The thrust may increase with β since Eq. (2) is proportional to β . Therefore, in order to obtain absolute value, the radial inhomogeneity should be taken into account. Other spatial inhomogeneity such as gradient in the z direction, violation of approximation far from the exit of the solenoid where B_r is comparable or greater than B_z would reduce thrust from the estimation given in this paper. Actual value should be obtained from more realistic numerical simulation in 2D or 3D geometry.

Second issue is the helicon plasma dispersion relation. In the helicon plasmas, it has been observed that the plasma density is proportional to the magnetic field strength. Therefore, when magnetic field is increased in order to maximize thrust, the thrust may increase due to the increase of the plasma density but not by optimization between two competing physical processes: REF shielding and R_D/r_0 .

Third issue is the inclusion of thrust due to other physical processes. Among of them, thermal thrust ($F_{th} = p\pi r_0^2$) is expected to be a dominant force. Here, variables of \dot{m} , and p are the mass flow rate of the plasma, and the plasma pressure, respectively. The contribution due to the thermal thrust is needed to be compared with the thrust by the Lissajous acceleration. Additionally, in the radial direction, the pressure force cancels force due to the diamagnetic current. However, the axial net force remains a positive value. The collision less fluid equation in MHD limit is written as

$$\rho \left(\frac{\partial}{\partial t} + \mathbf{u} \cdot \nabla \right) \mathbf{u} = -\nabla p + \mathbf{j} \times \mathbf{B}. \quad (4)$$

The plasma pressure is monotonically decreasing along z direction. Thus the force from the pressure term is positive and z component of the Lorentz force ($\mathbf{j}_\theta \times \mathbf{B}_r$) is positive. Therefore, the axial force due to the diamagnetic current [right-hand side of Eq. (4)] is none zero.

Fourth, the collisions have influences both on the \mathbf{j}_θ

and the REF penetration when the collision frequency approaches to ω for high plasma densities and/or high neutral densities. The effect of the collision should be considered in comparison with above issues.

Fifth, the REF penetration model is compared with PIC simulation at fixed ω_{RF} and L . In order to validate the model, comparison between the model and simulations for those variables are planned.

5. Summary

The electrodeless plasma thruster (Lissajous Helicon Plasma Accelerator) is studied by the analytical model which includes the electric field penetration into dense plasma. When the plasma density and the magnetic field are varied with other parameters are fixed, the thrust density is shown to be proportional to the ratio of the R_D/r_0 . However, the model shows that the thrust density eventually decreases with increase of the R_D/r_0 because of the reduction of the electrical field, which drives $\mathbf{E} \times \mathbf{B}$ drift motion for electrons. The reduction is due to an inhibition of the electron motion across the strong magnetic field. The degree of field penetration was found to be dominated by a dimensionless parameter (q) and is confirmed by the 1D PIC simulations.

Acknowledgements

This work is supported by the Grants-in-Aid for Scientific Research under Contract No. (S) 21226019 from the JSPS. The authors would like to acknowledge pioneering works by late Prof. Kyoichiro Toki.

- [1] K. Toki *et al.*, *Proceedings of the 28th International Electric Propulsion Conference* (Toulouse, France, 2003) IEPC 03-0168.
- [2] K. Toki *et al.*, *40th AIAA/ASME/SAE/ASEE Joint Propulsion Conference & Exhibit*, Fort Lauderdale (FL, USA, 2004) AIAA 2004-3935.
- [3] Robert G. JAHN, *Physics of Electric Propulsion*, MacGraw-Hill, Inc., New York, 1968.
- [4] C. Charles, *J. Phys. D: Appl. Phys.* **42**, 163001 (2009).
- [5] S. Shinohara *et al.*, *Phys. Plasmas* **16**, 057104 (2009).
- [6] J. Gilland, *AIAA/ASME/SAE/ASEE Joint Propulsion Conference and Exhibit, 34th* (Cleveland, OH, 1998) AIAA-1998-3934.
- [7] F.R. Chang-Díaz, *Sci. Am.* **283**, 90 (2000).
- [8] C. Charles, *Plasma Sources Sci. Technol.* **16**, R1 (2007).
- [9] H. Nishida *et al.*, *46th AIAA/ASME/SAE/ASEE Joint Propulsion Conference & Exhibit*, Nashville (TN, USA, 2010) AIAA2010-7013.
- [10] <http://www.txcorp.com/products/VORPAL/>